Sedimentary provenance constraints on the Cretaceous to Cenozoic palaeogeography of the western margin of the Jianhan Basin, South China

Xu Lin, Jing Liu-Zeng, Marc Jolivet, Weiming Liu, Feng Cheng, Haijin Liu, Lingling Li, Jixin Chen, Chengwei Hu, Xiaokang Chen

Journal Pre-proofs

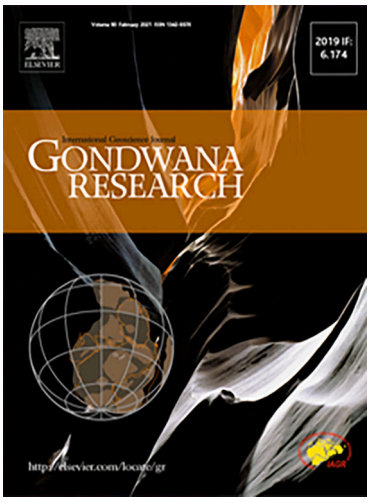

Sedimentary provenance constraints on the Cretaceous to Cenozoic palaeo-geography of the western margin of the Jianhan Basin, South China

Xu Lin, Jing Liu-Zeng, Marc Jolivet, Weiming Liu, Feng Cheng, Haijin Liu, Lingling Li, Jixin Chen, Chengwei Hu, Xiaokang Chen

PII: S1342-937X(23)00243-5
DOI: https://doi.org/10.1016/j.gr.2023.09.001
Reference: GR 3125

To appear in: *Gondwana Research*

Received Date: 4 July 2022
Revised Date: 8 August 2023
Accepted Date: 2 September 2023

Please cite this article as: X. Lin, J. Liu-Zeng, M. Jolivet, W. Liu, F. Cheng, H. Liu, L. Li, J. Chen, C. Hu, X. Chen, Sedimentary provenance constraints on the Cretaceous to Cenozoic palaeogeography of the western margin of the Jianhan Basin, South China, *Gondwana Research* (2023), doi: https://doi.org/10.1016/j.gr.2023.09.001

Sedimentary provenance constraints on the Cretaceous to Cenozoic palaeogeography of the western margin of the Jianhan Basin, South China

Xu Lin[a, g], Jing Liu-Zeng[b], Marc Jolivet[c*], Weiming Liu[d], Feng Cheng[e], Haijin Liu[f], Lingling Li[a], Jixin Chen[a], Chengwei Hu[a], Xiaokang Chen[a]

a. College of Civil Engineering and Architecture, China Three Gorges University, Yichang 443002, China

b. Institute of Surface-Earth System Science, Tianjin University, Tianjin 300072, China

c. Géosciences Rennes–UMR CNRS 6118, Université de Rennes, 35000 Rennes, France

d. CAS Key Laboratory of Mountain Hazards and Surface Process, Institute of Mountain Hazards and Environment, Chinese Academy of Sciences, Chengdu 610041, China

e. School of Earth and Space sciences, Peking University, Beijing 100871, China

f. School of Earth Sciences, East China University of Technology, Nanchang 330013, China

g. Collaborative Innovation Center for Geo-Hazards and Eco-Environment in Three Gorges Area, China Three Gorges University, Yichang 443002, China

[*] Corresponding author: Marc Jolivet, e-mail: marc.jolivet@univ-rennes1.fr

Abstract: Provenance analysis of sedimentary basins is a direct way to understand the uplift of orogenic belts, basin deposition, and evolution of large rivers. A series of Mesozoic and Cenozoic strata from the western Jianghan Basin provides key sedimentary archives for investigating the growth of the surrounding orogenic belts and the evolution of the Yangtze drainage. However, the provenance of these sediments remains unclear. In this study, we report U–Pb data for 1098 detrital zircons from the western Jianghan Basin. We combine these data with published zircon U–Pb ages of potential source areas, paleocurrent data, and paleomagnetic age constraints to reconstruct provenance areas and establish related mountain-building processes. All Cretaceous and Early Cenozoic samples show five major age peaks at 131–210, 432–461, 720–986, 1836–1908, and 2470–2552 Ma. We infer that these sediments are primarily derived from recycled sediments associated with the uplift of the western Jiangnan Orogen. The tectonic uplift of the Jiangnan orogenic belt in the Cretaceous and Early Cenozoic was mainly controlled by the subduction of the Pacific and Indian plates underneath Eurasia. The detritus in the current upper reaches of the Yangtze River did not enter the Jianghan

Basin before the Late Eocene (34 Ma). Early Pleistocene strata (1.2–0.7 Ma) show a distinct Cenozoic zircon U–Pb (41 Ma) peak age, which is mainly derived from the detrital sediments of the upper reaches of the Yangtze River. The combination of these data with published provenance tracing results for boreholes in the Jianghan Basin and Yangtze River Delta indicates that the Yangtze River was completely connected between 34 and 1.2 Ma. Such a long time interval may correspond to the tectonic uplift of the Tibetan Plateau and environmental changes during the Late Cenozoic.

Keywords: Detrital zircon U–Pb age, Paleogeography, Jianghan Basin, Jiangnan Orogen, Yangtze River

1. Introduction

Sedimentary basins and orogenic belts are paired components involved in the mass movement on Earth's surface. Sedimentary basins provide archives of geological records of detrital material that is transported by the rivers from orogenic belts (Liu-Zeng et al., 2008; Jolivet et al., 2010; Allen and Allen, 2013). It is very important to understand the source and sink system of sedimentary basins in geological times to reveal the deposition history of sedimentary basins and the tectonic evolution of adjacent orogenic belts (Tian et al., 2011; Li et al., 2016a; Jolivet et al., 2018; Cheng et al., 2021; Lin et al., 2022) and to construct the evolution of drainages connecting orogenic belts and sedimentary basins (Deng et al., 2018; Li et al., 2018; Wang et al., 2020a; Fu et al., 2021; Zhao et al., 2021a). However, inferring the sediment provenance from the final product, that is, the basin fill, is not straightforward because the detrital spectrum evolves as the sediment is transported along the pathway from the source to the basin (Weltje and von Eynatten, 2004; Clift et al., 2020).

The Jianghan Basin at the northern margin of the South China Block is sandwiched between the Qinling–Dabie and Jiangnan orogenic belts and has a clear basin–mountain boundary (Figure 1A). It is generally accepted that the Mesozoic and Cenozoic sedimentary strata in the Jianghan Basin recorded the far-field tectonism of the subduction of the Pacific and Indian plates underneath Eurasia (Shi et al., 2013; Dong et al., 2016; Wu et al., 2018). Mesozoic and Cenozoic strata in the western parts of the Jianghan Basin represent the most complete sedimentary sequence preserved and outcropped in the northern parts of the South China Block (Lei, 1987; Dai, 1997; Yao et al., 2015). Thus, studying Mesozoic and Cenozoic strata in the western Jianghan Basin provides information on the tectonics and river evolution of the South China Block (Xiang et al., 2007; Li, 2009a; Li et al., 2014; Yao et al., 2015; Dong et al., 2016; Wang et al., 2018; Kang et al., 2021). However, there is no consensus as to whether these sediments originated from the Qinling–Dabie orogenic belt in the north (Wang et al., 2009; She et al., 2012; Wu et al., 2017), Jiangnan orogenic belt in the south (Li, 2009a; Li, 2009b; Wang et al., 2013; Yao et al., 2015; Dong et al., 2016), both the Qinling and

Jiangnan orogenic belts (Yu et al., 2018), or the Huangling Anticline in the west (Shen et al., 2012a). This would suggest that for the detrital material, the proximal provenance areas in the Mesozoic and Cenozoic sedimentary strata from the western Jianghan Basin remain poorly defined.

The Yangtze River is the largest river in Asia, and it originates in the interior of the eastern Tibetan Plateau and drains Sichuan Basin, the Three Gorges, the Huangling Anticline and the Jianghan Basin before flowing into the East China Sea (Figure 1A). Richardson et al. (2010) proposed that the Yangtze River cut through the Three Gorges and entered the Jianghan Basin between 45–40 Ma based on low-temperature thermochronometric cooling ages of the bedrock of the Huangling Anticline. Based on inverse modelling of the long profile of a river channel and the low-temperature thermochronological data, Jiao et al. (2021) reconstructed the incision history of the Yangtze River near the eastern end of the Three Gorges area and suggested that the onset of the incision occurred in the Early Miocene (21–18 Ma). River terraces, which are well developed along the eastern Sichuan Basin and Three Gorges, formed from the Early to the Late Pleistocene (1.16–0.01 Ma). Therefore, Li et al. (2001) argued that the Three Gorges were cut at the beginning of the Early Pleistocene. This is controversial because the results of other studies suggested that the upper reaches of the Yangtze River were connected to the paleo-Red River system and began to flow eastward at 36 (Chen et al., 2017; He et al., 2021; Zheng et al., 2021; Zhang et al., 2021a), 20–18 Ma (Yan et al., 2012; McPhillips et al., 2016; Shen et al., 2016; Zhang et al., 2022) and 5.5 Ma (Su et al., 2019). In contrast, fission-track dating, U-Pb and trace-element analysis of detrital apatite, combined with U-Pb dating of detrital rutile and zircon, were employed to elucidate the capture of the Upper Yangtze River by the Middle Yangtze River after ca. 1.7–1.3 Ma. (Kong et al., 2012; Deng et al., 2021; Zhao et al., 2021b). However, these results have not been verified by Cenozoic sedimentary strata provenance tracing data from the western Jianghan Basin. Therefore, it remains unclear when the Yangtze River entered the Jianghan Basin. In other words, the geological information of the proximal and distal provenances recorded in the Mesozoic and Cenozoic strata of the western Jianghan Basin does not appear to have been well interpreted.

The comparative study of zircon U–Pb ages is a powerful tool for provenance tracing in sedimentary basins (Sircombe, 1999; Li et al., 2016a; Deng et al., 2018; Wang et al., 2018; Lin et al., 2021a; Wang et al., 2022a). Zircon U–Pb ages of bedrock and fluvial deposits around the Jianghan Basin have been widely reported (Lin et al., 2000; Ayers et al., 2002; Xiong et al., 2009; Chu et al., 2012; Zhao et al., 2013; Nie et al., 2016; Huang et al., 2021; Lin et al., 2021b). Detrital zircon data are abundant for the Yangtze River drainage (He et al., 2013; Liang et al., 2018; Lin et al., 2021b). This has laid a solid foundation for comparative studies of detrital zircon U–Pb ages in Meso–Cenozoic strata in the western Jianghan Basin. In this study, we present 1098 detrital zircon U–Pb ages obtained from 11 Cretaceous to Cenozoic sandstone and sand samples and combine them with the deposition time of the strata to determine the time of the provenance change. Published sandstone petrology and paleocurrent data (Li, 2009b; Yao et al., 2015; Wang et al., 2018) for Meso–Cenozoic strata from the western Jianghan Basin were used to

assist in determining the potential provenance area. The results contribute to the reconstruction of the paleogeographic evolution of the western Jianghan Basin and improve our understanding of the correlations among the exhumation of the intracontinental orogenic belt, sedimentary basin deposition, and big river evolution of the South China Block.

2. **Geological and geomorphic settings**

The Qinling–Dabie Orogen stretches across ~2000 km in central China (Figure 1A) and was formed by the collision between the North China Craton and South China Block during the Triassic (Dong et al., 2021). The granitic magmatism in the Qinling Shan can be divided into Neoproterozoic (979–711 Ma), Paleozoic (507–400 Ma), Early Mesozoic (250–185 Ma), and Late Mesozoic (160–100 Ma, Wang et al., 2015) stages. The Dabie Shan is characterised by widespread Triassic high-pressure/ultrahigh-pressure metamorphic rocks, which recorded the deep subduction of continental crust during the collision (Ayers et al., 2002; Dong et al., 2021). The granitic magmatism in the Dabie Shan can be divided into three main stages: Neoproterozoic (787 Ma), Early Mesozoic (235 Ma), and Late Mesozoic (132 Ma).

The Jiangnan Orogen (Figure 1A) has a width of ~120 km and extends NEE-SWW for ~1500 km. It is associated with the collision between the Yangtze and Cathaysia blocks along the Shaoxing–Jiangshan suture zone during the Early Neoproterozoic period (1.1–0.9 Ga) in South China Block (Li et al., 2014; Dong et al., 2016). The zircon U–Pb ages of the eastern segment of the Jiangnan Orogen (Mufu Shan) reflect the main magmatic events, which occurred at 987–823, 427, 218, and 154 Ma (He et al., 2013; Li et al., 2016b; Ji et al., 2017; Xin et al., 2017; Lin et al., 2021b). The magmatic zircons from the western parts of the Jiangnan Orogen (Xuefeng Shan, Wuling Shan) yield age clusters of 2700–1800, 900–700, 500–350, 300–150, and 120–100 Ma (Chu et al., 2012; Su et al., 2014; Ma et al., 2019; Lin et al., 2021b). The Huangling Anticline in the northern Yangtze Block was intruded by the 1.85 and 1.0–0.8 Ga granite in the north and south, respectively (Xiong et al., 2009; Zhang et al., 2009).

The Jianghan Basin (Figure 1A), with a total area of 28,000 km^2, evolved from a Middle Triassic foreland basin into a Cretaceous–Cenozoic rift basin in response to the multistage convergence and subsequent collision of the South China Block (Dai, 1997; Yao et al., 2015; Wu et al., 2018, Figure 1B). Mesozoic strata deposited in the western Jianghan Basin include the Early Cretaceous Shimen and Wulong formations and Late Cretaceous Luojingtan, Honghutao, and Paomagang formations (Lei, 1987; Li, 2009b; Yao et al., 2015, Figure 2, Figure 3A). The Shimen Formation (paleomagnetic age: 129–121 Ma, Dai, 1997) is dominated by thick brownish grey, massive breccia at the bottom, which is angular unconformable contact with the Ordovician or Permian limestone above. The middle and upper parts of the Shimen Formation consist of a thick grey-purple conglomerate with an imbricated gravel structure (Figure 3B) and the paleocurrent

direction is north or northeast (Li, 2009b, Figure 3A). The Wulong Formation (121–97.5 Ma, Dai, 1997) is mainly composed of brown-yellow fine- and medium-grained sandstone interbeded with siltstone, silty mudstone, and conglomerate (Figures 3C and D), which is in conformable contact with the Shimen Formation. The restored paleocurrent direction of the Wulong Formation is mainly directed from southwest to northeast (Li, 2009b, Figure 3A). The Luojingtan Formation (97.5–84.3 Ma, Dai, 1997) comprises a thick grey-brown massive conglomerate intercalated sandstone lens (Figures 3E and F), which is continuously deposited with the underlying Wulong Formation, and its provenance area is oriented in the southern direction (Yao et al., 2015). The Honghuatao Formation (84.3–72 Ma, Dai, 1997) mainly consists of orange–red massive fine grained sandstone (Figure 3G) and is in conformable contact with the Luojingtan Formation. The Paomagang Formation (72–65 Ma, Dai, 1997), which is in conformable contact with the Honghuatao Formation, is a brownish red and grey-white fine sandstone and siltstone interbedded with purple-red and sandy mudstone (Figure 3H).

The Gongjiachong Formation (65–54.9 Ma, Dai, 1997), which conforms with Paomagang Formation, is dominated by a brown-red thick massive conglomerate or pebbly sandstone at the bottom and brown-red silty mudstone interbedded with sandstone in the middle and upper parts (Figure 3 I). Its paleocurrent was distributed from south to north (Li, 2009b, Figure 3 A). The Yangxi Formation (54.9–50.5 Ma, Dai, 1997), which is in conformable contact with the Gongjiachong Formation, is composed of a set of greyish brown medium-thick-bedded argillaceous limestone intermixed with purplish-red mudstone and brownish-red sandstone (Figure 3J). The Cheyanghe Formation (50.5–42 Ma, Dai, 1997) is a light brown thick-bedded sandstone interbedded with thin reddish-brown mudstone and siltstone (Figure 3 K). It is in conformable contact with the Yangxi Formation. The cross bedding within the sandstone from the Cheyanghe Formation indicates that the paleo-river flowed northeastwards, consistent with the paleo-current direction recovered by the conglomerate (Li, 2009b; Wang et al., 2014a). The Pailoukou Formation (42–34 Ma, Dai, 1997), which is in conformable contact with the Cheyanghe Formation, is a light grey, thick layer of massive sandstone intermixed with grey-green muddy sandstone (Figure 3 L). The direction of the palaeocurrent indicated by the oblique bedding of the sandstone from the Pailoukou Formation is northeastward. The Yunchi Formation is characterised by a thick layer of yellowish gravel, which is well rounded and has a grain size of 2–10 cm (Figure 3 M). The gravel layer is in unconformable contact with underlying Eocene strata and its paleocurrent direction is south or southeast. Although Wang et al. (2018) assigned the Yunchi Formation to the Miocene, other researchers believe that it was formed in the Early Pleistocene based on electron spin resonance dating (ESR: 1.25–0.75 Ma; Xiang et al., 2007; Wei et al., 2020) and stratigraphic correlations (Kang et al., 2021).

3. Sampling and method

3.1 Sampling strategy

Sandstone and sand samples (2–5 kg) were collected from Mesozoic, Early Cenozoic, and Quaternary strata in the western Jianghan Basin. We collected one sample from the bottom (Y7) and one from the top (LJS-1) of the Wulong Formation. Late Cretaceous samples were obtained from the Luojingtan (Y6), Honghuatao (Y5), and Paomagang (Y4) formations. Samples Y3 and Y2 were obtained from the Gongjiachong and Cheyanghe formations. Samples Y1 and SZK-1 were collected from the bottom and top of the Pailoukou Formation, respectively. We took two samples from the bottom (YC-2) and top (YC-1) of the Yunchi Formation. As there are only a few sand beds in the Shimen and Yangxi formations, we were unable to collect samples from these strata in the field. Consequently, detrital zircon U-Pb age analysis was not performed for the Shimen and Yangxi formations. Specific information about the field sample collection is listed in Table 1.

3.2 Analytical methods

Zircon sorting was completed by the Hebei Langfang Chengxin Geological Service Co., Ltd., China. Under a binocular lens, zircon crystals were randomly selected to be fixed on epoxy resin, irrespective of their size, colour, or crystal form. In this study, ~90–110 grains from each sample were randomly picked for U–Pb dating. Zircon cathodoluminescence (CL) images were recorded and the grains were dated with a laser ablation microprobe (New Wave Research 213) coupled to a quadrupole inductively coupled plasma mass spectrometry (ICP-MS, Agilent 7800) at the Isotope Geology Laboratory of ChronusCamp, Brazil (Figure 4). Detailed analytical procedures are similar to those described by Shi et al. (2019). Concordia ages and diagrams were obtained using Isoplot/Ex (version 3.0, Ludwig, 2003). For frequency histograms and probability plots, only analyses within 100% ± 10% of concordance were used. All calculated ages were reported at the 95% confidence level. Grain ages younger than 1000 Ma were determined based on the $^{206}Pb/^{238}U$ values, whereas the ages of older grains were calculated based on the $^{207}Pb/^{206}Pb$ ratio (Sircombe, 1999).

Provenance area directly affects sandstone composition and plate tectonic activity controls the emergence and distribution of sandstone and other sedimentary rocks. Thus, the petrographic study of sedimentary archives is one of many strategies to deciphering geological history. Dickinson (1985) analyzed the composition of sandstones in multiple regions around the world to explore how the clastic composition of sandstones reflects the tectonic background of their source areas. The author performed a quantitative analysis, divided the sandstone debris components, and then compiled a triangular diagram based on the end tuple division, which is mainly divided into the QtFL, QmFLt, and QpLvLs types. Qt is the total number of quartz grains including monocrystalline quartz grains (Qm) and polycrystalline quartz fragments (Qp, including flint). F refers to the total number of feldspar grains including plagioclase (P) and potassium feldspar (K). L is the total number of debris particles composed of pyroclastic particles (Lv) and sedimentary rock debris particles (Ls). Lt represents polycrystalline debris, and is

composed of L and Qp. However, these diagrams can be further subdivided according to the needs and particularities of the study area. Over 300 grains were counted in each thin section using the Gazzi-Dickinson method and Ternary diagrams of the compositional trends were created.

Multi-dimensional scaling was used to produce a map-like plot in which the Euclidean distance between sample points was as close as possible to another measure of their distance. Furthermore, the detrital zircon U-Pb ages were subjected to Kolmogorov-Smirnov nonparametric tests (K-S test) among target samples and between samples and potential provenances. The K-S test calculates the maximum probability distance and has been previously validated for determining the potential provenance of target samples.

4. Results

CL images of representative zircons and age spots are shown in Figure 4. These zircon grains show a variety of shapes from prismatic crystals to oval grains, mainly with rounded corners. Note that most grains have Th/U ratios above 0.1 and below 10 and only a few grains have ratios below 0.1 (Figure 5). The CL images of the grains are characterised by oscillatory zoning (Figure 4), reflecting their magmatic origin. U–Pb isotopic ages with errors and relevant Supplementary Data are provided in Appendix A. The concordia plots for the 11 samples are shown in Figure 6.

The concordant detrital zircons from two sandstone samples (SZK-1 and Y1) from the Pailoukou Formation (E_2p) show broadly similar age patterns, with five major populations of 131–247, 263–321, 600–790, 1852–1910, and 2503–2536 Ma (Figures 7a–a′ and b–b′). The samples (Y2) from the Cheyanghe Formation (E_2c) exhibit U–Pb age spectra with predominant populations centred at 164–247, 428, 765, 1869, and 2536 Ma (Figures 7c–c′). The detrital zircons from the Early Cenozoic sample (Y3, E_1g) yield four major populations of 141–211, 308–432, 785, and 1861 Ma (Figure 7 d). The zircon U–Pb ages of the Paomagang Formation (K_2p) sandstone sample (Y4) show six major peak ages: 172, 238, 296, 461, 769, and 1869 Ma (Figures 7e–e′). Six peak ages were determined based on the detrital zircon U–Pb ages of samples from the Honghuatao Formation (K_2h, Y5): 131, 172, 222, 461, 774, and 1836 Ma (Figures 7f–f′). The U–Pb ages of detrital zircon from the Luojingtan Formation (K_2l, Y6) have predominant populations at 113–177, 210–307, 436–760, 1908–2539, and 3122 Ma (Figures 7g–g′). The detrital zircon U–Pb age populations of the two sandstone samples from the Wulong Formation (K_1w, Y7) of the Early Cretaceous are similar and concentrated at 161–164, 216–242, 307–308, 432–436, 720–825, 1844–1873, and 2470–2507 Ma (Figures 7h–h′ and i–i′). Zircon U-Pb ages of the two samples from the Yunchi Formation (Q_1y, YC1, YC2) have three predominant populations at 172–255, 444–774, and 1869–2495 Ma, a minor peak age at 41 Ma (Figures 7j–j′).

5. Discussion

5.1 Potential source areas of the western Jianghan Basin

5.1.1 Provenance area of Cretaceous strata

The majority of detrital zircon ages of Cretaceous samples can be grouped into similar age populations of 131, 161–164, 172–210, 432–461, 720–986, 1836–1908, and 2470–2552 Ma during the interval of 121–65 Ma (Figures 8Aa–e). The provenance of sedimentary material can be assessed by comparing detrital zircon U–Pb age compositions with areas or units that may have supplied sediment to the unit and region (Sircombe, 1999; Carter and Moss, 1999; Li et al., 2016a; Wang et al., 2018; Cheng et al., 2019; Lin et al., 2021a; Zheng et al., 2021). Major orogens and terranes around the Jianghan Basin are potential sources for these zircons, assuming that zircon-bearing rocks were exposed at that time. Four mountain ranges (Qinling Shan, Dabie Shan, Huangling Anticline, and Jiangnan Orogen) surrounding the Jianghan Basin have been proposed to be potential source areas that can contribute massive detritus to the western Jianghan Basin.

Bedrock and fluvial detrital zircon U–Pb ages of the Qinling Shan (Figure 9) fall into three peak ages of 216, 452, and 751 Ma (Nie et al., 2016; Liao et al., 2017; Lin et al., 2021b; Huang et al., 2021, Figure 8Af). Zircon U–Pb peak ages of Dabie Shan samples dominantly peak at 132, 235, and 787 Ma (Ayers et al., 2002; Zhao et al., 2008; Li et al., 2021; Lin et al., 2021b). Bedrock zircon U–Pb ages from the Huangling Anticline (Figure 8Ag) reveal a peak age of 813 Ma, followed by minor peaks at 1863 Ma (Xiong et al., 2009; Jiao et al., 2009; Zhang et al., 2009; Qiu et al., 2011; Zhao et al., 2013). Peak ages of 154, 442, and 823 Ma were obtained for samples from the eastern Jiangnan Orogen based on bedrock and fluvial zircon U–Pb ages (Lin et al., 2000; He et al., 2013; Wang et al., 2014b; Li et al., 2016b, 2016c; Ji et al., 2017; Xin et al., 2017; Lin et al., 2021b). Compared with Cretaceous strata in the western Jianghan Basin, the peak zircon ages of the Paleoproterozoic and Neoarchean from the above-mentioned potential areas are not significant, indicating the lack of a provenance relationship. However, the results of previous detrital zircon U–Pb dating and paleo-flow restoration indicated that Cretaceous sediments from the western parts of the Jianghan Basin originated from the Huangling Anticline in the west and Qinling Shan in the north (Shen et al., 2012a; Yu et al., 2020). These research sites are closer to the northwestern parts of the Jianghan Basin. This type of source-to-sink system shows several, rather than a single, source areas and simultaneously attributes sediments to the western Jianghan Basin (Shen et al., 2012b; Yu et al., 2020). In addition, the gravels of the Shimen, Wulong, and Luojingtan formations in this study are mainly limestone and dolomite, accounting for 90 %, 40 %, and 67 %, respectively (Li, 2009b; Wang et al., 2013; Yao et al., 2015). The Huangling Anticline and Qinling Shan mainly comprise granite outcrops, whereas metamorphic rocks constitute the main body of the Dabie Shan, which further rules out they non-existing provenance with Cretaceous strata analysed in this study. Zircon U–Pb dating and heavy mineral provenance tracing indicated that rivers in the western Huangling Anticline flowed westward into the Sichuan Basin during the Cretaceous (Li et al., 2018; Deng et al., 2018; Wang et al., 2021a; Zhao et al., 2021a). Therefore, we argue that there was no

provenance connection between the Mesozoic strata in the western Jianghan Basin and the Yangtze River during the Cretaceous.

The following pieces of evidence show that the western Jiangnan Orogen is a major potential source region for the Cretaceous strata of the western Jianghan Basin. First, compared with the peak ages of detrital zircon from Cretaceous strata of the western Jianghan Basin in this study (Figures 8Aa–e), the above-mentioned potential source areas (except for the Yangtze River Basin) lack significant Paleoproterozoic and Neoarchean peak ages. In contrast, bedrock and detrital zircon age signatures of the western Jiangnan Orogen show pronounced similarities with Cretaceous strata of the western Jianghan Basin because they share age populations of 129–131, 172–176, 210–223, 432–458, 720–924, 1811–1908, and 2470–2494 Ma (Chu et al., 2012; Ma et al., 2018; Su et al., 2018; Lin et al., 2021b). Second, Yao et al. (2015) analysed the carbon and oxygen isotopic compositions of the limestone gravel from the Wulong and Luojingtan formations and showed that they are derived from the western Jiangnan Orogen. Third, the paleocurrent direction of Cretaceous strata in the western Jianghan Basin is mainly directed northward or northeastward (Li, 2009b; Wang et al., 2013; Yao et al., 2015). The sedimentary environment is important for interpreting provenance and comparing source areas from a macroscopic perspective (Allen and Allen, 2013). Alluvial conglomerates in the Shimen and Luojingtan formations indicate a proximal source (Li, 2009b; Yao et al., 2015). On the MDS plots (Figures 10a–d), the four Cretaceous sandstone samples from the western Jianghan Basin show distinct affinities with the western Jiangnan Orogen. Therefore, as mentioned above, we can conclude that the detrital zircon grains in sandstone of Cretaceous strata in the southwestern parts of the Jianghan Basin are mainly derived from the western Jiangnan Orogen in the south.

5.1.2 Provenance area of Cenozoic strata

The zircon U–Pb age patterns of four sandstone samples from the Early Paleocene to Late Eocene (Figure 3) are similar to those of Cretaceous samples from the western Jianghan Basin (Figures 8Ba–d). By comparing the above-mentioned potential source areas with Paleogene sandstone samples in this study, the provenance areas of the western Jianghan Basin in the Paleogene period (65–34 Ma) were identified. The peak ages of the main populations in the Paleogene samples overlap with the age distributions recorded by detrital and bedrock zircon populations from the western Jiangnan Orogen. Several lines of evidence lead us to exclude the remaining potential source areas (Qinling Shan, Dabie Shan, Huangling Anticline, and eastern Jiangnan Orogen). First, the peak ages of 1852–1910 and 2503–2567 Ma are significant in the Paleogene strata in the western Jianghan Basin (Figures 8Ba–d) but absent or weak in the Qinling Shan (Figure 8Af), Dabie Shan (Figure 8Be), Huangling Anticline (Figure 8Bf), and eastern Jiangnan Orogen (Figure 8Bg). Furthermore, the prominent age populations of 428–469 Ma is significant in the western Jianghan Basin but absent in the Dabie Shan and Huangling Anticline. Second, the palaeocurrent directions of the Gongjiachong and Cheyanghe

formations are north and northeast, respectively, indicating that the provenance area was the southern part of the Jianghan Basin. Third, the closest provenance neighbour of the Gongjiachong, Cheyanghe, and Pailoukou formations in the MDS plots (Figures 10e–h) is the western Jiangnan Orogen, implying a potential source–sink relationship.

Four major peaks at 257, 782, 1852, and 2408 Ma and one minor peak at 41 Ma (Figure 8Ai) were identified in samples from the Yangtze River Basin at the western Jianghan Basin (Figure 9). Because the Yangtze River flows from Shigu Town to the Huangling Anticline (Figure 1A), mainly within the South China Block, its detrital zircon U–Pb peak ages are similar to those of the South China Block (He et al., 2013; Liang et al., 2018). However, because the Yangtze River passes through the Cenozoic magmatic body in the southeastern Tibetan Plateau (Zhang et al., 2019a), predominant age populations of zircons of 40–55 Ma are common in its fluvial sediments (He et al., 2013; Liang et al., 2018). By contrast, this Cenozoic peak age was not observed in Cenozoic strata in the western Jianghan Basin, indicating that there is no provenance link between the two areas. K-feldspar sand grains from the Cretaceous-Paleogene sequences in the western Jianghan Basin suggest that there was no large river like the Yangtze connecting the Tibetan Plateau to the Jianghan Basin at that time (Zhang et al., 2021b).

Because the zircon U–Pb age results obtained for samples YC1 and YC2 from the Yunchi Formation (Figure 8Bi) are similar, we combined the 180 age spectra into a single one for the discussion. Compared with the zircon U–Pb age compositions of samples from the Qinling Shan, Dabie Shan, Huangling Anticline, and eastern Jiangnan Orogen, zircons from the Yunchi Formation present distinct peak ages in the Paleoproterozoic and Neoarchean. The zircon U–Pb peak ages match those of samples from the upper reaches of the Yangtze River (Figure 8Bj). During the sedimentary period of the Yunchi Formation (1.2–0.75 Ma), the palaeocurrent direction changed from northward/northeastward into southeastward (Xiang et al., 2007), coinciding with the current mainstream of the Yangtze River. Based on the combination of the dating and MDS results, detrital zircons from the Yunchi Formation are not associated with the provenance of the above-mentioned potential source areas but originate from the upper reaches of the Yangtze River.

In summary, the samples from the Cretaceous and Paleocene succession in the study area generally have similar age patterns, which indicates that these strata belong to a continuous sedimentary system and share a common provenance area in the western Jiangnan Orogen. In contrast, the provenance of the western Jianghan Basin changed to the upper reaches of the Yangtze River during the Early Pleistocene, indicating the establishment of a provenance link between the Jianghan Basin and Tibetan Plateau during this period.

5.2 Tectonic implications and paleogeographic constraints for the South China Block

Detrital sediments within peripheral basins derived from adjacent orogenic belts accurately record the composition of their source regions and provide evidence of the evolution of orogenic belts and big rivers. Our results indicate that the western Jianghan Basin contains sediments that were derived from the western Jiangnan Orogen and upper reaches of the Yangtze River during the Meso–Cenozoic and Early Pleistocene, respectively. Therefore, we established a source–sink model for the western Jianghan Basin, revealing the provenance evolution from the Early Cretaceous (121 Ma) to the Early Pleistocene (1.2 Ma).

5.2.1 Cretaceous

Detrital zircon U–Pb dating (Deng et al., 2018; Li et al., 2018; Wang et al., 2021a) and the provenance of heavy mineral assemblages (Deng et al., 2018) indicate that the rivers derived from the western parts of the Huangling Anticline flowed into the Sichuan Basin from east to west during the Cretaceous (Figure 1B). This means that no large rivers flowed through the Sichuan and Jianghan basins at that time. The results of low-temperature thermochronological studies showed that extensive uplift and exhumation events (142–70 Ma) occurred in the western Jiangnan Orogen during the Cretaceous (Mei et al., 2010; Tang et al., 2014; Ge et al., 2016; Zheng et al., 2019; Chu et al., 2020). We thus attribute the zircon age distributions in Cretaceous clastic sediments within the western Jianghan Basin to the nearly synchronous denudation of the western Jiangnan Orogen. Correspondingly, the components of these sandstone samples suggest a sedimentary derivation from recycled and collision orogenic source areas according to the discriminant results of the QmFLt, QtFL, and QpLvLs plots (Li, 2019b; Yao et al., 2015; Wang et al., 2018, Figure 11). This is in line with high-energy alluvial- to fluvial-dominated coarse clastic deposits (Dai, 1997; Li, 2009a; Wang et al., 2013; Dong et al., 2016) that formed in the western Jianghan Basin during the same period. Such Cretaceous accumulations of coarse clastic deposits can also be observed in the Changtao Basin (Wu et al., 1979) and Yuanma Basin (Li et al., 2014) along the western Jiangnan Orogen. Hence, the above-mentioned evidence implies that the western Jiangnan Orogen had already been uplifted in the Cretaceous and provided the detrital sediments for the western Jianghan Basin. During the Cretaceous period, red bed deposits were widely distributed in South China Block (Li et al., 2014), mud cracks developed at the top of thin mudstone layers, and desert was extensively deposited in the Jianghan Basin (Yu et al., 2020), indicating that the paleoclimate was hot and dry. The arid climate is also evidenced by sporomorph fossils from most parts of the South China Block (Wang et al., 2022b). The oblique subduction of the Pacific Plate underneath the South China Block triggered the rifting of the Jianghan Basin during the Cretaceous (Dong et al., 2016; Wu et al., 2018). Therefore, tectonic activities have played the dominant role in the establishment of the basin–mountain coupling relationship between the western Jianghan Basin and western Jiangnan Orogen since the Cretaceous.

From a larger perspective, the results of previous thermochronological studies on

Mesozoic sedimentary rocks from the Eastern Sichuan Basin (Mei et al., 2010; Deng et al., 2013; Shi et al., 2016), Eastern Jiangnan Orogen (Shen et al., 2020; Wang et al., 2021b), and eastern parts of South China Block (Wang et al., 2020b; Suo et al., 2020) revealed that rapid exhumation took place during the Cretaceous. The formation of widespread coarse clastics from the Hengyang, Ganzhou, Ji'an, and Poyang basins (Figure 9) indicates that the basement rocks of eastern South China Block underwent rapid uplift and erosion during the Cretaceous (Luo et al., 1991; Li et al., 2014, Figure 12). These findings also coincide with the tectonic activity and low-angle subduction of the Pacific slab (Li et al., 2014). Overall, we infer that not only the entire Jiangnan orogenic belt but also other areas of the South China Block have suffered strong tectonic deformation, corresponding to the subduction of the Pacific Plate underneath the South China Block during the Cretaceous (Figure 1B).

5.2.2 Cenozoic

Integrated with detrital zircon U–Pb (Chen et al., 2017; Feng et al., 2021; Zheng et al., 2021; Wang et al., 2021a), heavy mineral (He et al., 2021), and K-feldspar Pb isotope (Zhang et al., 2021a) data, previous studies suggest that the upper reaches of the Yangtze River were separated from the Red River system at ~36–35 Ma. Furthermore, based on apatite fission-track and (U–Th)/He low-temperature thermochronology data from the Huangling Anticline, an enhanced cooling event occurred at 40 Ma. Richardson et al. (2010) proposed that the upper and middle reaches of the Yangtze River were connected in the Late Eocene. These studies imply that the provenance relationship between the southeastern margin of the Tibetan Plateau and the Jianghan Basin has been established during the Late Eocene. However, as mentioned above, the provenance tracing results of Paleogene sandstone samples from the western Jianghan Basin indicate that the source area was mainly derived from the western Jiangnan Orogen at 65–34 Ma (Figure 13A). In addition, the research results obtained for the Three Gorges of the Yangtze River (Jiao et al., 2021) and from cores of the Jianghan Basin (Yang et al., 2019; Zhang et al., 2021b) and lower Yangtze River delta (Jia et al., 2010; Zheng et al., 2013; Zhang et al., 2019b; Fu et al., 2021) reveal that the Yangtze River appeared in the Miocene or Pliocene.

There are pieces of evidences to indicate that the detrital materials in the western Jianghan Basin were mainly derived from the western Jiangnan Orogen corresponding to the far-field effects of the subduction of the Indian and Pacific plates underneath Eurasia. Firstly, the Pacific Plate began to subduct underneath Eastern Eurasia in the Early Paleocene, the direction changed from NNW to WNW at a reduced convergence rate of ~6.5 cm/yr (Maruyama et al., 1997; Müller et al., 2016). The Indian Plate collided with the Asian continent, with an increased convergent rate of ~16–17 cm/yr in the Early Paleocene (Müller et al., 2016; Suo et al., 2020). These two plate kinematics should have jointly affected South China Block, which experienced a compressional regime during

this period (Yin, 2010; Li et al., 2012; Dong et al., 2016; Tian et al., 2018; Wu et al., 2018). Secondly, low-temperature thermochronology data obtained on apatite and zircon indicate that the western Jiangnan Orogen experienced strong uplift from 60–40 Ma (Ge et al., 2016; Qiu et al., 2020). Coarse-grained alluvial fans and fluvial sediments in the western Jianghan Basin accumulated during this period. Thirdly, the QmFLt, QtFL, and QpLvLs plots show that the Early Paleogene sandstone deposited in the western Jianghan Basin belongs to recycled and collisional orogen materials (Li, 2009b; Yao et al., 2015; Wang et al., 2018, Figure 11). Moreover, the Jianghan Basin was not governed by a typical East Asian monsoon climate (Teng et al., 2019) but characterised by a dry and hot climate during the early Cenozoic (Dai, 1997; Zheng et al., 2011). Considering that the depocenter of the Jianghan Basin were accompanied by salt lake deposits in the Paleogene (Zheng et al., 2011; Wu et al., 2017; Teng et al., 2019), we conclude that the Jianghan Basin had not developed an outflow drainage system flowing through the basin at this time.

The detrital material of the Yunchi Formation is not related to the near-source orogenic belt of the Jianghan Basin but originated from the upper reaches of the Yangtze River between 1.2–0.7 Ma (Figure 13B). This indicates that the Yangtze River appeared in the Jianghan Basin during the Early Pleistocene, which agrees with previous provenance tracing results obtained for boreholes in the Jianghan Basin (Zhang et al., 2008; Wang et al., 2010; Shao et al., 2012; Sun et al., 2018) and Yangtze River Delta (Yang et al., 2009; Yue et al., 2018). In the Quaternary, large-scale orogenic movements around the Jianghan Basin ceased and the basin entered the stage of shrinkage and decline (Dai, 1997; Li, 2009b; Yao et al., 2015). The East Asian summer monsoon was in a phase of significant intensification between 1.2 and 0.7 Ma (Kissel et al., 2003; Wan et al., 2006). Therefore, the gravel layer of the Yunchi Formation deposited in the western Jianghan Basin reflects the transport of the Yangtze River affected by the East Asian summer monsoon during the Early Pleistocene.

6. Conclusions

The combination of the analysis of U–Pb ages of detrital zircon collected from Cretaceous–Cenozoic sedimentary rocks and available sandstone petrography, paleocurrent data, and paleomagnetic ages provides new information that can be used to constrain the source regions and tectonic evolution of the western Jianghan Basin in South China. In summary, the following main conclusions can be drawn:

(1) Due to the far-field effects of the subduction of the Pacific and Indian plates underneath Eurasia, the western Jiangnan Orogen was strongly uplifted during the Cretaceous and Early Cenozoic, contributing a large amount of clastic materials to the western Jianghan Basin. The provenance area of the western Jianghan Basin at this time mainly originated from the western Jiangnan Orogen. In the Early Pleistocene, the provenance area of the western Jianghan Basin changed to the Yangtze River, responding

to the strengthening of the East Asian summer monsoon.

(2) The upper reaches of the Yangtze River did not enter the western part of the Jianghan Basin during the Late Eocene (34 Ma). The provenance link between the Jianghan Basin and Tibetan Plateau was established through the Yangtze River in the Early Pleistocene (1.2 Ma). Combined with the published provenance tracing results obtained for boreholes in the Jianghan Basin and Yangtze River Delta, the connection of the whole Yangtze River Basin occurred between 34 and 1.2 Ma.

Acknowledgements

We would like to extend our sincere thanks to Dr. Licheng Wang and another anonymous reviewer for their careful review. We also want to thank editor Yongjiang Liu for his revision questions and suggestions. Many thanks to Yu Xiang from Fujian Normal University, who helped us greatly in the field sampling. We would like to thank Editage (www.editage.cn) for English language editing. This work was financially supported by the National Natural Science Foundation of China (grant numbers 41972212, 42030305) and the Research Foundation of Chutian Scholars Program of the Hubei Province (grant number 8210403).

References

Allen, P. A., Allen, J. R., 2013. Basin Analysis: Principles and Application to Petroleum Play Assessment. Third edition. Wiley-Blackwell, Oxford, 1-619.

Ayers, J. C., Dunkle, S., Gao, S., Miller, C. F. 2002. Constraints on timing of peak and retrograde metamorphism in the Dabie Shan ultrahigh-pressure metamorphic belt, east-central China, using U-Th-Pb dating of zircon and monazite. Chem. Geol. 186(3-4), 315-331.

Carter, A., Moss, S. J. 1999. Combined detrital-zircon fission-track and U-Pb dating: A new approach to understanding hinterland evolution. Geol. 27(3), 235-238.

Cen, Y., Peng, S., Kusky, T. M., Jiang, X., Wang, L. 2012. Granulite facies metamorphic age and tectonic implications of BIFs from the Kongling Group in the northern Huangling anticline. J Earth SCI-China. 23(5), 648-658.

Chen, Y., Yan, M., Fang, X., Song, C., Zhang, W., Zan, J., Zhang, D. 2017. Detrital zircon U-Pb geochronological and sedimentological study of the Simao Basin, Yunnan: Implications for the Early Cenozoic evolution of the Red River. Earth Planet Sc Lett. 476, 22-33.

Cheng, F., Garzione, C., Jolivet, M., Wang, W., Dong, J., Richter, F., Guo, Z. 2019. Provenance analysis of the Yumen Basin and northern Qilian Shan: Implications for the pre-collisional paleogeography in the NE Tibetan plateau and eastern termination of Altyn Tagh fault. Gondwana Res. 65, 156-171.

Cheng, F., Jolivet, M., Guo, Z., Wang, L., Zhang, C., Li, X. 2021. Cenozoic evolution of the Qaidam basin and implications for the growth of the northern Tibetan plateau: A review. Earth-Sci Rev. 103730.

Clift, P.D., Carter, A., Wysocka, A., Van Hoang, L., Zheng, H., Neubeck, N., 2020. A late Eocene-Oligocene through-flowing river between the upper Yangtze and south China Sea. G3. 21, e2020GC009046.

Chu, Y., Lin, W., Faure, M., Wang, Q., Ji, W. 2012. Phanerozoic tectonothermal events of the Xuefengshan Belt, central South China: Implications from U-Pb age and Lu-Hf determinations of granites. Lithos. 150, 243-255.

Chu, Y., Lin, W., Faure, M., Allen, M. B., Feng, Z. 2020. Cretaceous exhumation of the Triassic intracontinental Xuefengshan Belt: Delayed unroofing of an orogenic plateau across the South China Block?. Tectonophysics. 793, 228592.

Dai, S. Z. 1997. Petroleum Geology of Jianghan Saline Basin. Petroleum Industry Publishing House, Beijing, 1-223(in Chinese with English abstract).

Deng, B., Liu, S. G., Li, Z. W., Jansa, L. F., Liu, S., Wang, G. Z., Sun, W. 2013. Differential exhumation at eastern margin of the Tibetan Plateau, from apatite fission-track thermochronology. Tectonophysics. 591, 98-115.

Deng, B., Chew, D., Jiang, L., Mark, C., Cogné, N., Wang, Z., Liu, S. 2018. Heavy mineral analysis and detrital U-Pb ages of the intracontinental Paleo-Yangzte basin: Implications for a transcontinental source-to-sink system during Late Cretaceous time. Geol Soc Ambull. 130(11-12), 2087-2109.

Deng, B., Chew, D., Mark, C., Liu, S., Cogné, N., Jiang, L., Li, J. 2021. Late Cenozoic drainage reorganization of the paleo-Yangtze river constrained by multi-proxy provenance analysis of the Paleo-lake Xigeda. Geol Soc Ambull. 133(1-2), 199-211.

Dickinson, W.R., 1985. Interpreting provenance relations from detrital modes of sandstones, in Zuffa, G.G., ed., Provenance of Arenites: Dordrecht, Netherlands, Springer, North Atlantic Treaty Organization (NATO) Advanced Study Institute (ASI) Series C: MPS. 148, 333-361.

Dong, Sh. W., Zhang, Y. Q., Zhao, Y., Zhang, F. Q., Yang, Zh. Y., Chen, X. H. 2016. Mesozoic-Cenozoic tectonic evolution and dynamic analysis of the Chinese continent. Science Press, Beijing, 1-714(in Chinese with English abstract).

Dong, Y., Sun, S., Santosh, M., Zhao, J., Sun, J., He, D., Zhang, G. 2021. Central China Orogenic Belt and amalgamation of East Asian continents. Gondwana Res. 100, 131-194.

Feng, Y., Song, C., He, P., Meng, Q., Wang, Q., Wang, X., Chen, W. 2021. Detrital

zircon U-Pb geochronology of the Jianchuan Basin, southeastern Tibetan Plateau, and its implications for tectonic and paleodrainage evolution. Terra Nova. 33(6), 560-572.

Fu, X., Zhu, W., Geng, J., Yang, S., Zhong, K., Huang, X., Xu, X. 2021. The present-day Yangtze River was established in the late Miocene: Evidence from detrital zircon ages. J Asian Earth Sci. 205, 104600.

Garzanti, E. 2019. Petrographic classification of sand and sandstone. Earth-Sci Rev. 192, 545-563.

Ge, X., Shen, C., Selby, D., Deng, D., Mei, L. 2016. Apatite fission-track and Re-Os geochronology of the Xuefeng uplift, China: Temporal implications for dry gas associated hydrocarbon systems. Geology, 44(6), 491-494.

He, M., Zheng, H., Clift, P. D. 2013. Zircon U-Pb geochronology and Hf isotope data from the Yangtze River sands: Implications for major magmatic events and crustal evolution in Central China. Chemical Geology, 360, 186-203.

He, M., Zheng, H., Clift, P. D., Bian, Z., Yang, Q., Zhang, B., Xia, L. 2021. Paleogene sedimentary records of the paleo-Jinshajiang (Upper Yangtze) in the Jianchuan Basin, Yunnan, SW China. Geochemistry, Geophysics, Geosystems, 22(6), e2020GC009500.

Hubei Bureau of Geology and Mineral Resources. 1991. 1: 40000 geological map of Yichang area. Geological Publishing House, Beijing, 1(in Chinese with English abstract).

Huang, H., He, D., Li, D., Li, Y. 2021. Zircon U-Pb ages and Hf isotope analysis of Neoproterozoic Yaolinghe Group sedimentary rocks in the Chengkou area, South Qinling: Provenance and paleogeographic implications. Precambrian Research, 355, 106088.

Ji, W., Lin, W., Faure, M., Chen, Y., Chu, Y., Xue, Z. 2017. Origin of the Late Jurassic to Early Cretaceous peraluminous granitoids in the northeastern Hunan province (middle Yangtze region), South China: Geodynamic implications for the Paleo-Pacific subduction. J Asian Earth Sci. 141, 174-193.

Jia, J., Zheng, H., Huang, X., Wu, F., Yang, S., Wang, K., He, M. 2010. Detrital zircon U-Pb ages of Late Cenozoic sediments from the Yangtze delta: Implication for the evolution of the Yangtze River. Chin Sci Bull. 55(15), 1520-1528.

Jiao, W., Wu, Y., Yang, S., Peng, M., Wang, J. 2009. The oldest basement rock in the Yangtze Craton revealed by zircon U-Pb age and Hf isotope composition. Sci China Earth Sci. 52(9), 1393-1399.

Jiao, R., Yang, R., Yuan, X. 2021. Incision history of the Three Gorges, Yangtze River

constrained from inversion of river profiles and low-temperature thermochronological data. J Geophys Res-Earth. 126(3), 2020JF005767.

Jolivet, M., Dominguez, S., Charreau, J., Chen, Y., Li, Y., Wang, Q. 2010. Mesozoic and Cenozoic tectonic history of the central Chinese Tian Shan: Reactivated tectonic structures and active deformation. Tectonics. 29(6),1-30.

Jolivet, M., Barrier, L., Dauteuil, O., Laborde, A., Li, Q., Reichenbacher, B., Guo, Z. 2018. Late Cretaceous–Palaeogene topography of the Chinese Tian Shan: New insights from geomorphology and sedimentology. Earth Planet Sc Lett. 499, 95-106.

Kang, C., Li, C. A., Wei, C., Zhang, Y., Jiang, H., Li, Y., Guo, R. 2021. Heavy mineral assemblage variation in late Cenozoic sediments from the Middle Yangtze River Basin: Insights into basin sediment provenance and evolution of the Three Gorges Valley. Minerals. 11(10), 1056.

Kissel, C., Laj, C., Clemens, S., Solheid, P. 2003. Magnetic signature of environmental changes in the last 1.2 Myr at ODP Site 1146, South China Sea. Mar Geol. 201(1-3), 119-132.

Kong, P., Zheng, Y., Caffee, M. W. 2012. Provenance and time constraints on the formation of the first bend of the Yangtze River. G3, 13(6), 1-15.

Lei, Y. Z. 1987. Stratigraphic excursion guidebook in the Yangtze Gorges Area. Geological Publishing House, Beijing, 64-79(in Chinese with English abstract).

Li, P., Liu, X. S., Li, Zh. W., Pan, Y. Sh., Xie, M. Y., Xue, Y. G. 1966. Mesozoic and Cenozoic geological structure development in North and South China. Science Press, Beijing, 1-105(in Chinese with English abstract).

Li, J., Xie, S., Kuang, M. 2001. Geomorphic evolution of the Yangtze Gorges and the time of their formation. Geomorphology. 41(2-3), 125-135.

Li, Zh. F. 2009a. A study on the sedimentary paleogeography of the Late Jurassic and Cretaceous in the middle Yangtze area. Master thesis of China University of Geosciences (Beijing), 1-65.

Li, J. 2009b. Relationship between characteristics of paleocurrent and basin-filling evolution of Upper Jurassic-Paleogene in the middle Yangtze Area. Master thesis of China University of Geosciences (Beijing), 1-72.

Li, J., Zhang, Y., Dong, S., Hailong, L. 2012. Late Mesozoic-Early Cenozoic deformation history of the Yuanma Basin, central South China. Tectonophysics. 570, 163-183.

Li, J., Zhang, Y., Dong, S., Johnston, S. T. 2014. Cretaceous tectonic evolution of South China: A preliminary synthesis. Earth-Sci Rev. 134, 98-136.

Li, Y., He, D., Chen, L., Mei, Q., Li, C., Zhang, L. 2016a. Cretaceous sedimentary basins in Sichuan, SW China: Restoration of tectonic and depositional environments. Cretaceous Res. 57, 50-65.

Li, X. C., Wang, A. D., Wan, X. J. Li, Q. Z., Lin, L. F. 2016b. Tracing the stream sediment of the Ganjiang River(Nanchang Section): Constraint from the detrital zircon U-Pb isotope evidence. Geoscience. 30(3), 514-527(in Chinese with English abstract).

Li, J., Dong, S., Zhang, Y., Zhao, G., Johnston, S. T., Cui, J., Xin, Y. 2016c. New insights into Phanerozoic tectonics of south China: Part 1, polyphase deformation in the Jiuling and Lianyunshan domains of the central Jiangnan Orogen. J Geophys-Sol Ea. 121(4), 3048-3080.

Li, Y., He, D., Li, D., Lu, R., Fan, C., Sun, Y., Huang, H. 2018. Sedimentary provenance constraints on the Jurassic to Cretaceous paleogeography of Sichuan Basin, SW China. Gondwana Res. 60, 15-33.

Li, W. T., Jiang, S. Y., Fu, B., Liu, D. L., Xiong, S. F. 2021. Zircon Hf-O isotope and magma oxidation state evidence for the origin of Early Cretaceous granitoids and porphyry Mo mineralization in the Tongbai-Hong'an-Dabie orogens, Eastern China. Lithos. 106281.

Liao, X. Y., Wang, Y. W., Liu, L., Wang, C., Santosh, M. 2017. Detrital zircon U-Pb and Hf isotopic data from the Liuling Group in the South Qinling belt: provenance and tectonic implications. J Asian Earth Sci. 134, 244-261.

Liang, Z. W., Gao, S., Hawkesworth, C. J., Wu, Y. B., Storey, C. D., Zhou, L., Liu, X. M. 2018. Step-like growth of the continental crust in South China: evidence from detrital zircons in Yangtze River sediments. Lithos. 320, 155-171.

Lin, W., Faure, M., Monié, P., Schärer, U., Zhang, L., Sun, Y. 2000. Tectonics of SE China: new insights from the Lushan massif (Jiangxi Province). Tectonics. 19(5), 852-871.

Lin, X., Liu, J., Wu, Z., Li, C., Liu, H. 2021a. Study on borehole provenance tracing and fluvial sediment diffusion in the Bohai Sea: Double constraints from detrital zircon U-Pb age and in-situ geochemical element of apatite grains. J Geomech. 27(2), 304-316(in Chinese with English abstract).

Lin, X., Zhao, X., Wu, Z., Liu, H., Li, L. L., Chen, J. X. 2021b. Detrital zircon U-Pb ages characteristics of main rivers around Jianghan Basin and provenance-tracing implication. Acta Geoscientia Sinica. 43(1), 73-81(in Chinese with English abstract).

Lin, X., Jolivet, M., Liu-Zeng, J., Cheng, F., Wu, Z., Tian, Y., Chen, J. 2022. The formation of the North Qilian Shan through time: clues from detrital zircon

fission-track data from modern river sediments. Geosciences. 12(4), 1-20.

Liu-Zeng, J., Tapponnier, P., Gaudemer, Y., Ding, L. 2008. Quantifying landscape differences across the Tibetan plateau: Implications for topographic relief evolution. J Geophys Res-Earth. 113(F4),1-26.

Ludwig, K. R. 2003. User's manual for IsoPlot 3.0. A geochronological toolkit for Microsoft Excel, 71.

Luo, T., Duan, J. Z., Jiang, J. G., Xu, Z. Y., Shi, Q. W. 1991. Geological conditions and prospective evaluation of hydrocarbon formation in Dongting-Poyang-Mayang Basin. Jianghan Petroleum Administration Bureau, Wuhan, 1-174(in Chinese with English abstract).

Ma, H., Wang, Y., Huang, Y., Xie, Y. 2019. Three-stage Mesozoic intracontinental tectonic evolution of South China recorded in an overprinted basin: evidence from stratigraphy and detrital zircon U-Pb dating. Geol Mag, 156(12), 2085-2103.

Maruyama, S., Isozaki, Y., Kimura, G., Terabayashi, M. 1997. Paleogeographic maps of the Japanese Islands: Plate tectonic synthesis from 750 Ma to the present. Isl Arc, 6(1), 121-142.

McPhillips, D., Hoke, G. D., Liu-Zeng, J., Bierman, P. R., Rood, D. H., Niedermann, S. 2016. Dating the incision of the Yangtze River gorge at the First Bend using three-nuclide burial ages. GRL. 43(1), 101-110.

Mei, L. F., Liu, Z, Q., Tang, J. G., Shen, Ch. B. Fan, Y. F. 2010. Mesozoic Intra-continental progressive deformation in Western Hunan-Hubei-Eastern Sichuan provinces of China: Evidence from apatite fission track and balanced cross-section. ERSC, 35(2), 161-174(in Chinese with English abstract).

Müller, R. D., Seton, M., Zahirovic, S., Williams, S. E., Matthews, K. J., Wright, N. M., Cannon, J. 2016. Ocean basin evolution and global-scale plate reorganization events since Pangea breakup. Annu Rev Earth Pl Sc. 44, 107-138.

Nie, H., Yao, J., Wan, X., Zhu, X. Y., Siebel, W., Chen, F. 2016. Precambrian tectonothermal evolution of South Qinling and its affinity to the Yangtze Block: Evidence from zircon ages and Hf-Nd isotopic compositions of basement rocks. Precambrian Res. 286, 167-179.

Qiu, X. F., Ling, W. L., Liu, X. M., Kusky, T., Berkana, W., Zhang, Y. H., Liu, C. X. 2011. Recognition of Grenvillian volcanic suite in the Shennongjia region and its tectonic significance for the South China Craton. Precambrian Res. 191(3-4), 101-119.

Qiu, L., Yan, D. P., Tang, S. L., Chen, F., Gong, L. X., Zhang, Y. X. 2020. Cenozoic exhumation of the Neoproterozoic Sanfang batholith in South China. J Geol Soc

738 London. 177(2), 412-423.

739 Richardson, N. J., Densmore, A. L., Seward, D., Wipf, M., Yong, L. 2010. Did incision
740 of the Three Gorges begin in the Eocene?. Geology. 38(6), 551-554.

741 Sircombe, K. N. 1999. Tracing provenance through the isotope ages of littoral and
742 sedimentary detrital zircon, eastern Australia. Sediment Geol. 124(1-4), 47-67.

743 Su, J., Dong, S., Zhang, Y., Li, Y., Chen, X., Cui, J. 2014. Detrital zircon geochronology
744 of pre-Cretaceous strata: tectonic implications for the Jiangnan Orogen, South
745 China. Geol Mag. 151(6), 975-995.

746 Su, J., Dong, S., Zhang, Y., Ma, L., Chen, X. 2018. Geochronology, geochemistry, and
747 tectonic implications of Jishou Cretaceous diabase, western Xuefengshan tectonic
748 zone in South China. Geol J. 53(3), 1186-1199.

749 Su, H., Dong, M., Hu, Z. 2019. Late Miocene birth of the Middle Jinsha River revealed
750 by the fluvial incision rate. Global Planet Change. 183, 103002.

751 Sun, X., Kuiper, K. F., Wang, J., Tian, Y., Vermeesch, P., Zhang, Z., Wijbrans, J. R.
752 2018. Geochronology of detrital muscovite and zircon constrains the sediment
753 provenance changes in the Yangtze River during the late Cenozoic. Basin
754 Res. 30(4), 636-649.

755 Shao, L., Yuan, S., Kang, C., Wang, J., Li, T. 2012. Neodymium isotopic variations of
756 the late Cenozoic sediments in the Jianghan Basin: Implications for sediment
757 source and evolution of the Yangtze River. J Asian Earth Sci. 45, 57-64.

758 She, Z., Ma, C., Wan, Y., Zhang, J., Li, M., Chen, L., Gao, J. 2012. An Early Mesozoic
759 transcontinental palaeoriver in South China: evidence from detrital zircon U-Pb
760 geochronology and Hf isotopes. J Geol Soc London. 169(3), 353-362.

761 Shen, C. B., Donelick, R. A., O'Sullivan, P. B., Jonckheere, R., Yang, Z., She, Z. B., Ge,
762 X. 2012a. Provenance and hinterland exhumation from LA-ICP-MS zircon U-Pb
763 and fission-track double dating of Cretaceous sediments in the Jianghan Basin,
764 Yangtze block, central China. Sediment Geol. 281, 194-207.

765 Shen, C., Mei, L., Peng, L., Chen, Y., Yang, Z., Hong, G. 2012b. LA-ICPMS U–Pb
766 zircon age constraints on the provenance of Cretaceous sediments in the Yichang
767 area of the Jianghan Basin, central China. Cretaceous Res. 34, 172-183.

768 Shen, X., Tian, Y., Li, D., Qin, S., Vermeesch, P., Schwanethal, J. 2016. Oligocene-Early
769 Miocene river incision near the first bend of the Yangze River: Insights from
770 apatite (U-Th-Sm)/He thermochronology. Tectonophysics. 687, 223-231.

771 Shen, C., Hu, D., Min, K., Yang, C., Zeng, X., Fu, H., Ge, X. 2020. Post-Orogenic
772 Tectonic Evolution of the Jiangnan-Xuefeng Orogenic Belt: Insights from

Multiple Geochronometric Dating of the Mufushan Massif, South China. J Earth Sci-China. 31(5), 905-918.

Shi, W., Dong, S. W., Ratschbacher, L., Tian, M., Li, J. H., Wu, G. L. 2013. Meso-Cenozoic tectonic evolution of the Dangyang Basin, north-central Yangtze Craton, central China. Int Geol Rev. 55(3), 382-396.

Shi, H., Shi, X., Glasmacher, U. A., Yang, X., Stockli, D. F. 2016. The evolution of eastern Sichuan basin, Yangtze block since Cretaceous: constraints from low temperature thermochronology. J Asian Earth Sci. 116, 208-221.

Shi, G., Soares, C. J., Shen, C., Wang, H., Yang, C., Liang, C., Liu, M. 2019. Combined detrital zircon fission track and U-Pb dating of the Late Paleozoic to Early Mesozoic sandstones in the Helanshan, western Ordos fold-thrust belt: Constraints for provenance and exhumation history. Journal of Geodynamics, 130, 57-71.

Suo, Y. H., Li, S. Z., Cao, X., Wang, X. Y., Somerville, I., Wang, G., Wang, P., Liu, B. 2020. Mesozoic-Cenozoic basin inversion and geodynamics in East China: a review. Earth-Sci Rev.103357.

Tang, S. L., Yan, D. P., Qiu, L., Gao, J. F., Wang, C. L. 2014. Partitioning of the Cretaceous Pan-Yangtze Basin in the central South China Block by exhumation of the Xuefeng Mountains during a transition from extensional to compressional tectonics?. Gondwana Res. 25(4), 1644-1659.

Teng, X., Fang, X., Kaufman, A. J., Liu, C., Wang, J., Zan, J., Piatak, N. M. 2019. Sedimentological and mineralogical records from drill core SKD1 in the Jianghan Basin, Central China, and their implications for late Cretaceous–early Eocene climate change. J Asian Earth Sci. 182, 103936.

Tian, Y., Kohn, B. P., Zhu, C., Xu, M., Hu, S., Gleadow, A. J. 2012. Post-orogenic evolution of the Mesozoic Micang Shan Foreland Basin system, central China. Basin Res. 24(1), 70-90.

Tian, Y., Kohn, B. P., Qiu, N., Yuan, Y., Hu, S., Gleadow, A. J., Zhang, P. 2018. Eocene to Miocene Out-of-Sequence deformation in the Eastern Tibetan Plateau: Insights from shortening structures in the Sichuan Basin. J Geophys Res-Sol Ea. 123(2), 1840-1855.

Vermeesch, P. 2013. Multi-sample comparison of detrital age distributions. Chem Geol. 341, 140-146.

Vermeesch, P., Resentini, A., Garzanti, E. 2016. An R package for statistical provenance analysis. Sediment Geol. 336, 14-25.

Wan, S., Li, A., Clift, P. D., Jiang, H. 2006. Development of the East Asian summer

monsoon: Evidence from the sediment record in the South China Sea since 8.5 Ma. Palaeogeogr Palaeocl. 241(1), 139-159.

Wang, Y., Zhao, G., Xia, X., Zhang, Y., Fan, W., Li, C., Li, S. 2009. Early Mesozoic unroofing pattern of the Dabie Mountains (China): Constraints from the U-Pb detrital zircon geochronology and Si-in-white mica analysis of synorogenic sediments in the Jianghan Basin. Chem Geol. 266(3-4), 231-241.

Wang, J., Li, C. A., Yang, Y., Shao, L. 2010. Detrital zircon geochronology and provenance of core sediments in Zhoulao Town, Jianghan plain, China. J Earth Sci-China. 21(3), 257-271.

Wang, P., Liu, S. F., Zheng, H. B., Wang, K., Gao, T. J., Pan, F., Li, W. P., Jiang, Ch. X. Chen, Y. L., Yang, X. S. 2013. Late-orogenic arcuate fold-thrust belts in northern Yangtze area: Structural characteristics and basin evolution. J Palaeogeog-English. 15(6), 819-838(in Chinese with English abstract).

Wang, P., Zheng, H., Chen, L., Chen, J., Xu, Y., Wei, X., Yao, X. 2014a. Exhumation of the Huangling anticline in the Three Gorges region: Cenozoic sedimentary record from the western Jianghan Basin, China. Basin Res. 26(4), 505-522.

Wang, L. X., Ma, C. Q., Zhang, C., Zhang, J. Y., Marks, M. A. 2014b. Genesis of leucogranite by prolonged fractional crystallization: a case study of the Mufushan complex, South China. Lithos. 206, 147-163.

Wang, X., Wang, T., Zhang, C. 2015. Granitoid magmatism in the Qinling orogen, central China and its bearing on orogenic evolution. Sci China Earth Sci. 58(9), 1497-1512.

Wang, P., Zheng, H., Liu, S., Hoke, G. 2018. Late Cretaceous drainage reorganization of the middle Yangtze River. Lithosphere-US. 10(3), 392-405.

Wang, L., Shen, L., Liu, C., Ding, L. 2020a. Evolution of the paleo-Mekong River in the Early Cretaceous: Insights from the provenance of sandstones in the Vientiane Basin, central Laos. Palaeogeogr Palaeocl. 545, 109651.

Wang, Y., Wang, Y., Li, S., Seagren, E., Zhang, Y., Zhang, P., Qian, X. 2020b. Exhumation and landscape evolution in eastern South China since the Cretaceous: New insights from fission-track thermochronology. J Asian Earth Sci. 191, 104239.

Wang, L., Shen, L., Liu, C., Chen, K., Ding, L., Wang, C. 2021a. The Late Cretaceous source-to-sink system at the eastern margin of the Tibetan Plateau: Insights from the provenance of the Lanping Basin. Geosci Front. 12(3), 101102.

Wang, Y., Bai, Q., Tian, Z., Lu, S., Li, J., Zhou, Y., Jiang, C. 2021b. Exhumation history of late Mesozoic intrusions in the Tongling-Xuancheng area of the Lower

Yangtze region, eastern China: Evidence from zircon (U-Th)/He and apatite fission track thermochronology. Ore Geol Rev. 104220.

Wang, L., Ding, L., Garzanti, E., Shen, L., Nulay, P., Siritongkham, N. 2022a. Mid-Cretaceous drainage reorganization and exorheic to endorheic transition in Southeast Tibet. Sediment Geol. 439, 106221.

Wang, J. Y., Li, X. H., Li, L. Q., Wang, Y. D. 2022b. Cretaceous climate variations indicated by palynoflora in South China. Palaeoworld. 31(3), 507-520.

Wei, C., Voinchet, P., Zhang, Y., Bahain, J. J., Liu, C., Kang, C., Sun, X. 2020. Chronology and provenance of the Yichang Gravel Layer deposits in the Jianghan Basin, middle Yangtze River Valley, China: Implications for the timing of channelization of the Three Gorges Valley. Quatern In. 550, 39-54.

Weltje, G. J., von Eynatten, H. 2004. Quantitative provenance analysis of sediments: review and outlook. Sediment Geol. 171(1-4), 1-11.

Wu, P., Yang, Zh. Q. 1979. Cretaceous-Cenozoic lithofacies paleogeography and ore-bearing properties in Central and South China. Geological Publishing House, Beijing, 1-65(in Chinese with English abstract).

Wu, Y., Zheng, Y. 2004. Genesis of zircon and its constraints on interpretation of U-Pb age. Chinese Sci Bull. 49(15), 1554-1569.

Wu, L., Mei, L., Liu, Y., Luo, J., Min, C., Lu, S., Guo, L. 2017. Multiple provenance of rift sediments in the composite basin-mountain system: Constraints from detrital zircon U-Pb geochronology and heavy minerals of the early Eocene Jianghan Basin, central China. Sediment Geol. 349, 46-61.

Wu, L., Mei, L., Paton, D. A., Guo, P., Liu, Y., Luo, J., Wen, H. 2018. Deciphering the origin of the Cenozoic intracontinental rifting and volcanism in eastern China using integrated evidence from the Jianghan Basin. Gondwana Res. 64, 67-83.

Xiang, F., Zhu, L., Wang, C., Zhao, X., Chen, H., Yang, W. 2007. Quaternary sediment in the Yichang area: Implications for the formation of the Three Gorges of the Yangtze River. Geomorphology. 85(3-4), 249-258.

Xiong, Q., Zheng, J., Yu, C., Su, Y., Tang, H., Zhang, Z. 2009. Zircon U-Pb age and Hf isotope of Quanyishang A-type granite in Yichang: signification for the Yangtze continental cratonization in Paleoproterozoic. Chinese Sci Bull. 54(3), 436-446.

Xin, Y., Li, J., Dong, S., Zhang, Y., Wang, W., Sun, H. 2017. Neoproterozoic post-collisional extension of the central Jiangnan Orogen: Geochemical, geochronological, and Lu-Hf isotopic constraints from the ca. 820-800 Ma magmatic rocks. Precambrian Res. 294, 91-110.

Yao, J. M., Ju, Y. T., Lao, H. G., Dong, G. Y., Li, Sh. Y. 2015. Sedimentary characteristics from Late Jurassic to Neogene in the Middle Yangtze Region. Wuhan University Press, Wuhan, 1-123(in Chinese with English abstract).

Yan, Y., Carter, A., Huang, C. Y., Chan, L. S., Hu, X. Q., Lan, Q. 2012. Constraints on Cenozoic regional drainage evolution of SW China from the provenance of the Jianchuan Basin. G3. 13(3), Q03001.

Yang, S., Wang, Z., Guo, Y., Li, C., Cai, J. 2009. Heavy mineral compositions of the Changjiang (Yangtze River) sediments and their provenance-tracing implication. J Asian Earth Sci. 35(1), 56-65.

Yang, C., Shen, C., Zattin, M., Yu, W., Shi, S., Mei, L.2019. Provenances of Cenozoic sediments in the Jianghan Basin and implications for the formation of the Three Gorges. Int Geol Rev. 61(16), 1980-1999.

Yin, A. 2010. Cenozoic tectonic evolution of Asia: A preliminary synthesis. Tectonophysics. 488(1-4), 293-325.

Yu, X., Liu, C., Wang, C., Xu, H. 2018. Provenance of rift sediments in a composite basin-mountain system: constraints from petrography, whole-rock geochemistry, and detrital zircon U-Pb geochronology of the Paleocene Shashi Formation, southwestern Jianghan Basin, central China. Int J Earth Sci. 107(8), 2741-2766.

Yu, X., Liu, C., Wang, C., Li, F., Wang, J. 2020. Eolian deposits of the northern margin of the South China (Jianghan Basin): Reconstruction of the Late Cretaceous East Asian landscape in central China. Mar Petrol Geol. 117, 104390.

Yue, W., Jin, B., Zhao, B. 2018. Transparent heavy minerals and magnetite geochemical composition of the Yangtze River sediments: Implication for provenance evolution of the Yangtze Delta. Sediment Geol. 364, 42-52.

Zhao, Z. F., Zheng, Y. F., Wei, C. S., Chen, F. K., Liu, X., Wu, F. Y. 2008. Zircon U–Pb ages, Hf and O isotopes constrain the crustal architecture of the ultrahigh-pressure Dabie orogen in China. Chem Geol. 253(3-4), 222-242.

Zhao, J. H., Zhou, M. F., Zheng, J. P. 2013. Neoproterozoic high-K granites produced by melting of newly formed mafic crust in the Huangling region, South China. Precambrian Res. 233, 93-107.

Zhao, X. M., Wu, N. W., Niu, Z. J. Mo, W. R. 2019. Geological map of the People's Republic of China (Central China, 1:1500000). Geological Publishing House, Beijing, 1-109(in Chinese with English abstract).

Zhao, X. D., Zhang, H. P., Hetzel, R. Kirby, E., Duvll, R. A., Whipple, X. K., Xiong, J. G., Li, Y. F., Pang, J. Z., Wang, Y., Wang, P., Liu, K., Ma, P. F., Zhang, B., Li, X. M., Zhang, J. W., Zhang, P. Z. 2021a. Existence of a continental-scale river

system in eastern Tibet during the late Cretaceous-early Palaeogene. Nat Commun. 12, 7231.

Zhao, X., Zhang, H., Tao, Y., Wang, Y., Pang, J., Ma, Y., Xiong, J. 2021b. Pliocene to Early Pleistocene drainage reorganization in eastern Tibet inferred from detrital zircons. GRL. 48(20), e2021GL094563.

Zhang, Y., Li, C. A., Wang, Q., Chen, L., Ma, Y., Kang, C. 2008. Magnetism parameters characteristics of drilling deposits in Jianghan Plain and indication for forming of the Yangtze River Three Gorges. Chinese Sci Bull. 53(4), 584-590.

Zhang, S. B., Zheng, Y. F., Zhao, Z. F., Wu, Y. B., Yuan, H., Wu, F. Y. 2009. Origin of TTG-like rocks from anatexis of ancient lower crust: geochemical evidence from Neoproterozoic granitoids in South China. Lithos. 113(3-4), 347-368.

Zhang, Y., Huang, W., Zhang, Y., Poujol, M., Guillot, S., Roperch, P., Guo, Z. 2019a. Detrital zircon provenance comparison between the Paleocene-Eocene Nangqian-Xialaxiu and Gongjue basins: New insights for Cenozoic paleogeographic evolution of the eastern Tibetan Plateau. Palaeogeogr Palaeocl. 533, 109241.

Zhang, J., Wan, S., Clift, P. D., Huang, J., Yu, Z., Zhang, K., Zhang, X. 2019b. History of Yellow River and Yangtze River delivering sediment to the Yellow Sea since 3.5 Ma: Tectonic or climate forcing?. Quaternary Sci Rev. 216, 74-88.

Zhang, Z., Daly, J. S., Yan, Y., Lei, C., Badenszki, E., Sun, X., Tian, Y. 2021a. No connection between the Yangtze and Red rivers since the late Eocene. Mar Petrol Geol. 129, 105115.

Zhang, Z., Daly, J. S., Tyrrell, S., Sun, X., Badenszki, E., Li, Y., Yan, Y. 2021b. Formation of the Three Gorges (Yangtze River) no earlier than 10 Ma. Earth-Sci Rev. 216, 103601.

Zhang, D., Cao, K., Yuan, X., Wang, G., van der Beek, P. 2022. Late Oligocene-early Miocene Origin of the First Bend of the Yangtze River explained by thrusting-induced river reorganization. Geomorphology. 108303.

Zheng, H., Jia, D., Chen, J., Wang, P. 2011. Did incision of the Three Gorges begin in the Eocene? Comment. Geology. 39(9), 244.

Zheng, H., Clift, P. D., Wang, P., Tada, R., Jia, J., He, M., Jourdan, F. 2013. Pre-miocene birth of the Yangtze River. PNAS. 110(19), 7556-7561.

Zheng, C., Xu, C., Brix, M. R., Zhou, Z. 2019. Evolution and provenance of the Xuefeng intracontinental tectonic system in South China: Constraints from detrital zircon fission track thermochronology. J Asian Earth Sci. 176, 264-273.

951 Zheng, H., Clift, P. D., He, M., Bian, Z., Liu, G., Liu, X., Jourdan, F. 2021. Formation of
952 the First Bend in the late Eocene gave birth to the modern Yangtze River,
953 China. Geology. 49(1), 35-39.

954

955 Figure 1. (A) Map showing the major tectonic blocks and location of the study area
956 (modified from Li et al., 2014; Dong et al., 2016). Abbreviations: SXJS: Shaoxing–
957 Jiangshan suture zone; DY: Dayong fault; TLF: Tanlu fault. (B) Cartoon figure showing
958 the formation mechanism of the Cretaceous–Early Cenozoic in the Jianghan Basin
959 (modified from Li et al., 2014). The backarc extension was associated with the rollback
960 or retreat of the subducted paleo-Pacific slab.

961

962 Figure 2. Geological map delineating the distribution of Cretaceous to Cenozoic strata
963 and sample locations (modified from a 1:1500000 geological map; Zhao et al., 2019).

964

965 Figure 3. (A) Cretaceous and Cenozoic stratigraphic units and typical photographs
966 showing the sampling horizons at the western Jianghan Basin. The magnetostratigraphic
967 and ESR ages were obtained from Dai (1997), Xiang et al. (2007), and Wei et al. (2020).
968 Paleocurrent data are cited from Li (2009b), Yao et al. (2015), and Wang et al. (2013).
969 (B) Massive breccia and thick conglomerate with a clast size ranging from 5 to 30 cm in
970 an alluvial fan deposit in the Shimen Formation. (C–D) Thick coarse sandstone with
971 siltstone, silty mudstone, and conglomerate and cross-bedding developed in sandstone
972 strata in braided fluvial deposits of the Wulong Formation. (E–F) Thick conglomerate
973 with sizes ranging from 2 to 20 cm intercalated sandstone is alluvial fan deposits of the
974 Luojingtan Formation. (G–H) Honghuatao and Paomagang formations composed of
975 massive fine sandstone, siltstone, and mudstone in a shallow lacustrine deposit. (I)
976 Gongjiachong Formation mainly containing thick conglomerate, pebbly sandstone, and
977 mudstone in alluvial fan facies. (J) Carbonate lacustrine facies strata developed in the
978 Yangxi Formation with argillaceous bands. (K–L) Massive sandstones, mudstones, and
979 siltstones developed in the Cheyanghe and Pailoukou formations and planar
980 cross-stratification used to determine the paleocurrent directions, indicating a meandering
981 river delta facies. (M) Yunchi Formation consisting of alluvial fan sedimentary facies
982 with thick gravel and sandy lens deposits. The size of the gravel is well rounded and
983 sorted, ranging from 2–10 cm.

984

985 Figure 4. Representative CL images of detrital zircon from the western Jianghan Basin
986 showing the internal structure and morphology. Yellow circles indicate the U–Pb
987 analysis spots.

Figure 5. Plot of Th versus U of concordant detrital zircons used in this study. Th/U values above 0.4 indicate zircons with an igneous origin, whereas values below 0.1 represent metamorphic zircons (Wu and Zheng, 2004).

Figure 6. U – Pb concordia diagrams of detrital zircon collected from the Jianghan Basin constructed using ISOPLOT (Ludwig, 2003).

Figure 7. Distribution of detrital zircon U – Pb ages of Cretaceous – Cenozoic sediments (a – j) from the western Jianghan Basin. Detrital zircon ages ranging from 0 – 500 Ma are shown on the right (a′ – j′).

Figure 8. Zircon U – Pb age probability density plots of (A) Cretaceous (a – e) and (B) Cenozoic (a – d, i) sediments in the western Jianghan Basin compared with age spectra from potential source regions (Af: Qinling Shan; Ag: Huangling Anticline; Ah: eastern Jiangnan Orogen; Ai: western Jiangnan Orogen; Aj: Yangtze River; Be: Dabie Shan). Note that the Cenozoic zircon peak age (41 Ma) only appears in Yangtze River (Aj) and Quaternary samples (Bi).

Figure 9. Map showing the marked positions of cited zircon age data in potential source areas. Abbreviations: HJR = Hanjiang River, QJR = Qingjiang River, LSR = Lishui River, YJR = Yuangjiang River, ZJR = Zijiang River, XJR = Xiangjiang River, GJR = Ganjiang River; HL = Huangling Anticline, WLS = Wuling Shan; WJN = West Jiangnan Orogen, EJN = East Jinangnan Orogen. Data sources: Yangtze River (He et al., 2013; Liang et al., 2018), Qinling Shan (Wang et al., 2015; Nie et al., 2016; Liao et al., 2017; Lin et al., 2021b; Huang et al., 2021), Dabie Shan (Ayers et al., 2002; Zhao et al., 2008; Li et al., 2021; Lin et al., 2021b), Huangling Anticline (Xiong et al., 2009; Jiao et al., 2009; Zhang et al., 2009; Qiu et al., 2011; Cen et al., 2012; Zhao et al., 2013), eastern Jiangnan Orogen (Lin et al., 2000; He et al., 2013; Wang et al., 2014b; Li et al., 2016b; Li et al., 2016c; Ji et al., 2017; Xin et al., 2017; Lin et al., 2021b), western Jiangnan Orogen (Chu et al., 2012; Ma et al., 2018; Su et al., 2018; Lin et al., 2021b). Yellow squares, white diamonds, and white circles represent river samples cited from He et al.(2013), Li et al.(2016), and Lin et al. (2021b), respectively.

Figure 10. Multidimensional scaling (MDS) plot for Cretaceous (a – d) and Cenozoic (e – i) detrital zircon data generated following methods outlined by Vermeesch et al. (2016). The solid and dashed lines mark the nearest and second nearest neighbours, respectively. Abbreviations: DB: Dabie Shan, EJN: eastern Jiangnan Orogen, WJN: western Jiangnan Orogen, QL: Qinling Shan, YR: Yangtze River, HL: Huangling Anticline.

Figure 11. Triangular plots of detrital components for the studied sandstones (Dickinson, 1985). (A) QmFLt plot; (B) QtFL plot; (C) QpLvLs plot. Qm: monocrystalline quartz; Qp: polycrystalline quartz; Qt: total quartz (Qm+Qp); F: total feldspar; Ls: sedimentary lithic grains; Lv: volcanic lithic grains; L: total nonquartzose lithic grains (Ls+Lv); Lt: total lithic grains (L+Qp). Data sources: Wulong and Luojingtan Formation: Li (2009b), Yao et al. (2015); Honghuatao and Cheyanghe Formation: Wang et al. (2018).

Figure 12. Correlation section showing the characteristics of sedimentary facies of Cretaceous and Cenozoic strata surrounding the Jiangnan orogenic belt. Numbers 1 – 7 represent the corresponding positions in Figure 9. Data for the Changtao (1) and Poyang (7) basins were obtained from Li et al. (1966) and Luo et al. (1991), respectively. Data for the Yuanma (3), Hengyang (4), Ganzhou (5), and Ji'an (6) basins were taken from Li et al. (2014).

Figure 13. Reconstruction of the basin – mountain and river distribution maps from the Late Cretaceous to Early Cenozoic (A) and Early Pleistocene (B) in the Yangtze River Basin.

Table 1. Collected sampling point information

Table 1. Collected sampling point information

Sample No.	Strata (Fm.)	GPS		Nature of sample
Y7	Wulong	30°38′17″N	111°19′55″ E	sandstone
LJS-1	Wulong	30°41′02″N	111°16′55″	sandstone

			E	
Y6	Luojingtan	30°33′18″N	111°23′21″ E	sandstone
Y5	Honghuatao	30°31′27″N	111°23′17″ E	sandstone
Y4	Paomagang	30°16′29″N	111°31′08″ E	sandstone
Y3	Gongjiachong	30°16′48″N	111°31′14″ E	sandstone
Y2	Cheyanghe	30°15′12″N	111°34′37″ E	sandstone
Y1	Pailoukou	30°17′09″N	111°36′39″ E	sandstone
SZK-1	Pailoukou	30°18'33"N	111°37'32"E	sandstone
YC-2	Yunchi	30°33'10"N	111°27'39"E	sand
YC-1	Yunchi	30°31'50"N	111°26'04"E	sand

Tectonic activities control the sedimentary processes in the western Jianghan Basin.

The Jiangnan orogenic belt is the main provenance area of western Jianghan Basin.

The Yangtze River enters the Jianghan Basin between 34 Ma and 1.2 Ma.

We declare that the data in this article are true and reliable.